Brazilian Journal of Physics, vol. 22, no. 1, March, 1992

Beam Profile Manipulation in a Self-Defocusing Nonlinear Media

J. Miguel Hickmann, A.S.L. Gomes and Cid B. Araujo
Departamento de Física, Universidade Federal de Pernambuco, 50739, Recife-PE, Brasil

Received January 31, 1992

We describe optical profile manipulations by another beam through spatial cross-phase modulation in a nonlinear medium. Spatial modulation instability, induced focusing and induced all-optical waveguide are demonstrated.

I. Introduction

Nonlinear pulse propagation in bulk media can lead to substantial modifications in the temporal, spectral or spatial characteristics of a given input pulse. It has been realized earlier that when a pulse propagates in a Kerr-type medium[1] there is a perfect analogy between the spectro-temporal behavior of the pulseshape with the spatial behavior of the pulse spatial profile[2]. This analogy has been realized back in 1969[3], in optical pulse compression, and fully exploited more recently[4].

The Kerr effect leads to the self-phase modulation (SPM) of a pulse, which affects its spectral width by broadening it, without affecting the pulse temporal duration. The amount of spectral broadening depends on the pulse intensity, interaction length and the nonlinear index of refraction, n_2, which can be positive or negative and is a characteristic of the medium. When acting on the spatial domain, the Kerr effect leads to self-focusing, if $n_2 > 0$, or self defocusing, if $n_2 < 0$, of a beam propagating in a nonlinear material. An inherent effect acting on the beam profile is the diffraction, which always broadens the beam width. In the time domain, the group velocity dispersion is responsible for the pulsewidth broadening, and even though it can be positive or negative, always leads to pulse broadening. One natural question then arises: can one control the pulse duration and/or profile such as to avoid pulse distortion? The solution relies on the generation of "solitons" - either temporal solitons or spatial solitons. Optical solitons have been predicted back in 1973[5] and first experimentally verified in the time domain seven years later[6], while spatial optical solitons were predicted in 1964[7] and first verified in 1985[8]. Physically, optical temporal solitons exist due to the balance between a positive (negative) nonlinearity and negative (positive) group velocity dispersion and are described by the nonlinear Schrodinger equation, which can be written in a normalized form as[9] :

$$i\frac{\partial A}{\partial Z} = \frac{1}{2}\beta_2\frac{\partial^2 A}{\partial T^2} - \gamma|A|^2 A \qquad (1)$$

where A is the pulse envelope, β_2 is proportional to the group velocity dispersion, T is the time in the coordinate system moving with tlie group velocity, Z is the coordinate along the propagation direction in the nonlinear medium and y = $\frac{\omega_0 n_2}{cA_{eff}}$ where ω_0 is the center frequency, c is the speed of light, A_{eff} is the effective core are and n_2 is the nonlinear index of refractive. For optical fibers (where optical solitons were first observed) $n_2 > 0$ and β_2 can be positive ($\lambda < 1.3\mu m$) or negative ($\lambda > 1.3\mu m$). In optical fibers, solitons exist for $n_2 > 0$ and $\beta_2 < 0$.

A similar equation describes the spatial solitons, and can be written as:

$$i\frac{\partial A}{\partial Z} = -\frac{1}{2}\frac{1}{K}\frac{\partial^2 A}{\partial x^2} - K\frac{n^2}{n_0}|A|^2 A \qquad (2)$$

where A is the envelope amplitude, K is the light wavevector and x is the transverse spatial coordinate. Rigorously, one should write two transverse dimensions, but eq.(2) can be well applied for spatial solitons in planar waveguides, as demonstrated by Aitchison et al.[10].

So far we have described a few self-effects of the light propagating in a nonlinear medium, whereby a single-beam or single pulse is required. Other self-effects include the self-bending of a beam profile, first proposed in 1969[11] and recently observed using CW beams[12]. One can catalogue the analogy between space-time in nonlinear pulse propagation, as in Table 1, where the physical effects occurring in each domain are compared side-by-side. References are given to quantities not mentioned in this text. A new question can then be gut forward: what happens when two pulses (or two beams) of different wavelengths propagate together through a nonlinear medium? In the time domain, it has been shown both theoretically and experimentally, in bulk media[13] and optical fibers[14] that the derivation of the propagation equation leads to a pair of coupled NLSE from which a term due to a cross-phase modulation (XPM) arises. It is because of this term that one pulse (or beam) affects the other through the nonlinearity, even though there is no energy change. Sev-

eral features due to **XPM** have been demonstrated in the temporal domain including modulational instability induced by XPM[15], picosecond pulse generation[16], optical wave breaking and pulse compression[17]. In the spatial domain, at least two demonstration have been described so far, which is the induced bending and focusing[18,19]. In what follows, we describe experimental results demonstrating recent predictions of spatially induced focusing and bending[20], induced modulational instability[21] and, furthermore, we will show that an all-optical channel waveguide can be created through XPM, which may sustain a beam propagating without distortion of its profile. An important point to stress here is that all these phenomena occur in a self-defocusing medium, which is particularly intriguing for observation of a iòcusing effect[1].

II. Spatial Cross-Phase Modulation

The XPM effect can be described by a set of propagation equations whose derivation can be found in ref. [9,13]. In the spstial domain and in the paraxial approximation, these equations take the form[20] :

$$\frac{\partial A_1}{\partial Z} - \frac{i}{2K_1}\left[\frac{\partial^2 A_1}{\partial x^2} + \frac{\partial^2 A_1}{\partial y^2}\right] = \frac{iK_1 n_2}{n_{01}}(|A_1|^2 + 2|A_2|^2)A_1 \quad (3)$$

$$\frac{\partial A_2}{\partial Z} - \frac{i}{2K_2}\left[\frac{\partial^2 A_2}{\partial x^2} + \frac{\partial^2 A_2}{\partial y^2}\right] = \frac{iK_2 n_2}{n_{02}}(|A_2|^2 + 2|A_1|^2)A_2 \quad (4)$$

where the indexes 1,2 indicate the two beams, $n_{01,2}$ are the corresponding refractive indexes and all the other terms have the same meaning as in eq. (2). Equations (3) and (4) can be numerically solved by the split-step Fourier method (see ref. 9). To simplify the equations, only one trsnsverse coordinate is taken into account, which is experimentally justified by the use of planar waveguide geornetries. Several regimes regarding the two beams have been analyzed in [20,21], and here we will be only concerned with the pump-probe regime, i.e., one strong beam which suffers nonlinear self-effects and induces, through XPM, nonlinear effects in the probe beam, and a weak beam which does not affect itself neither the strong pump beam.

If we consider both the pump and probe bearns to have Gaussian profiles with half-widths, W_0 and W_0', with wavelength ratio $\lambda_1/\lambda_2 \sim 0.9$, and choose n_2 to be negative, the effect of the strong beam on the weak beam is shown to be determined by how much the beams profile overlap. For total overlap of both beams, it has been predicted that the probe beam broadens, but siniultaneously it creates spatial sidebands, as shown in figure 1, calculated using the parameters of ref. [21]. If the bearns are partially overlappeci, the result is totally different, and a shift concomitant with a narrowing of the pulse profile is predicted, as shown in fig. 2, calculated using the parameters of ref. [20]. Even though the medium is self-defocusing to both pump and probe beams, figure 2 shows that a profile compression occurs, and this is due to the combination of both XPM, which distorts the probe bearn profile, and the fact that there is a spatial mismatch between pump and probe beam at the input of the sample. The pump beam itself defocuses, and the portion of the probe bearn contained in the wings of the pump beam profile sees a negative phase-front curvature, which leads to a focusing of the probe beam. In the next section, we describe the experimental details and results for the observation of such effects.

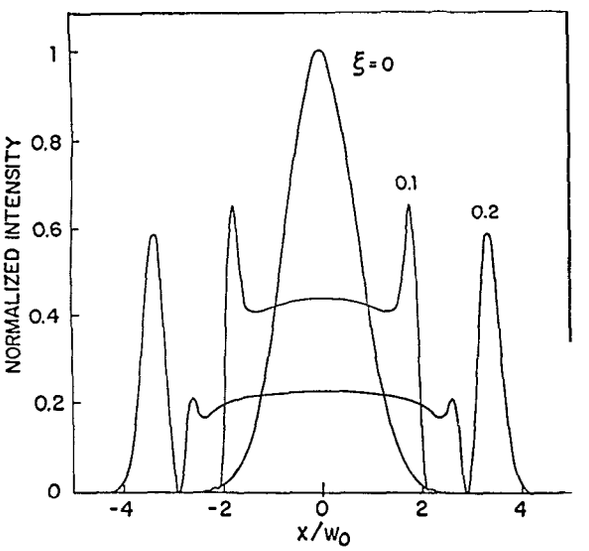

Figure 1.: Evolution of probe beam profiles for different propagation distances ($\xi = 0; 01; 0.2$). The input bearns (widths: W_0) are Gaussian and their overlap is perfect (after ref. 21).

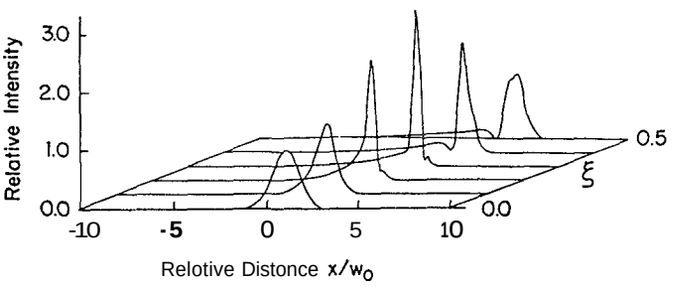

Figure 2.: Evolution of probe beam profiles over a distance $\xi = 0 - 0.5$. The input beams are Gaussian, have the same width W_0 and are separated by W_0 (after ref. 20).

III. Experimental Results

The experimental scheme used is shown in fig. 3. The second harmonic of a Q-switched and mode-locked

Table I - Space-Time Analogy

Spectro-Temporal domain	(Ref.)	**Spatial Domain**	(Ref.)
Propagation direction r	[1]	Propagation direction z	[1]
Time T	[1]	Transverse position x or y	[1]
Temporal envelope $\left\{A(t) \propto \exp\left(-\frac{t^2}{2t_0^2}\right)\right\}$	[1]	Profile $\left\{(A(x) \propto \exp\left(-\frac{x^2}{2W_0^2}\right)\right\}$	[1]
Dispersion	[1]	Diffraction	[1]
Compression	[1]	Focusing	[1]
Broadening	[1]	Defocusing	[1]
Self-phase modulation	[1]	Self-focusing/defocusing	[1]
Spectrum	[1,20]	Far field profile	[1,20]
Cross-phase modulation	[20,21]	Induced focusing/defocusing	[20,21]

Nd:YAG laser was used. Each Q-switched burst consists of about 20 pulses of $80ps$ duration separated by $10ns$. The available average (peak) power was 200 $mW(\sim 360kW)$ and the Q-switch repetition rate was $200Hz$. The laser beam was split through a beam splitter BS1 ($\sim$ 10% reflection at $532nm$) and the weakest part was used to generate, through stimulated Raman scattering (22) in a 14m long monomode fiber, radiation Stokes shifted to longer wavelenghs. A filter is employed to separate the wavelength corresponding to the first Stokes at $544nm$, which was used as the weak probe beam. The remaining strong beam at $\lambda_2 = 532nm$ was spatially filtered and combined, through the beam splitter BS2, to copropagate with the probe beam. A careful adjustment of the temporal overlap between the pulses was done. The power of the pump beam was controlled using a $\lambda/2$ waveplate/polarizer (P) combination before the spatial filter (SF). The beams overlap on the sample was adjusted using the output objectives of the fibe ($\times 40$) and the spatial filter ($\times 60$). The measured beams waist at the sample position was $90\mu m$ for the pump and $120\mu m$ for the probe beam. The Rayleigh lengths were $\sim$ 5cm and $8cm$, respectively.

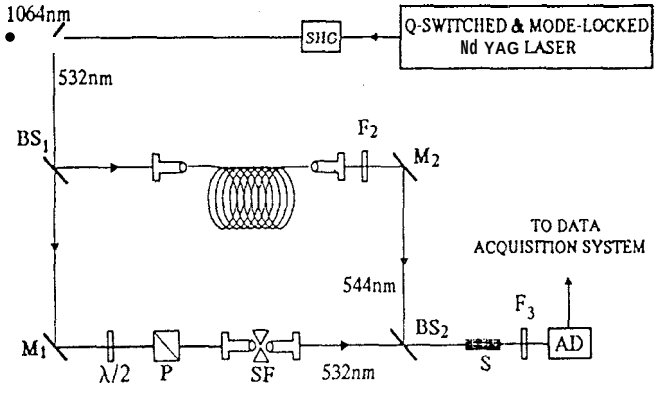

Figure 3.: Experimental set-up. S is the nonlinear sample used (Corning glass CS 3-69). M_1 and M_2 are mirrors. The other symbols are explained in the text.

A commercially available semiconductor doped glass

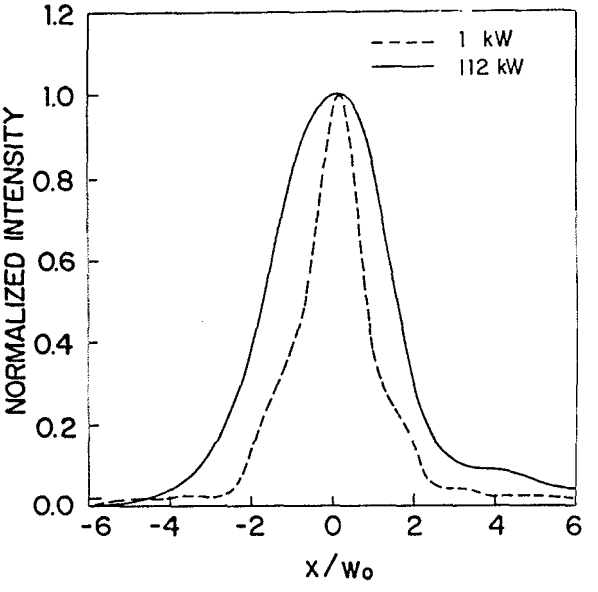

Figure 4.: Evolution of the pump beam profile exhibiting self-defocusing after propagation through the sample (Corning glass CS 3-69; length = 5cm).

(Corning CS 3-69), $5cm$ long, was used as the nonlinear sample. This material, well known for its large nonlinear response $\chi^{(3)} \sim 10^{-8} esu$ has been well characterized [22-25]. For the wavelengths used in this work $Re\chi^{(3)}$ is negative and much larger than its imaginary part [25].

The beams profile were analyzed using a linear 1024 - photodetector-array, whose output was sent to a digital oscilloscope and transfered to a micro-computer. The diode array was placed $\sim$ 1cm behind the sample in order to measure the near-field profile of the transmitted beams. The probe beam was weak enough not to be affected by self-defocusing, while the pump beam is strong enough to be self-defocused. The filter F_3 was used to block the pump beam.

Figure 4 shows the pump beam profile after propagation through the sample. The presented results, obtained for two incident pump intensities, show a spatial broadening by a factor of 2 due to the negative nonlinear refractive index of the sample. For intermediate powers smaller broadening factors were observed.

To examine the XPM effect imposed on the probe laser by the strong beam, we analyzed the probe beam profile as a function of the pump intensity and as a function of the spatial overlap between both beams. The two beams were aligned to copropagate along the sample. A carefiil adjustment of the beams overlap allowed to move the pump laser across the profile of the probe beam, such as to either properly overlap, or to overlap only in the wings of the beams profile.

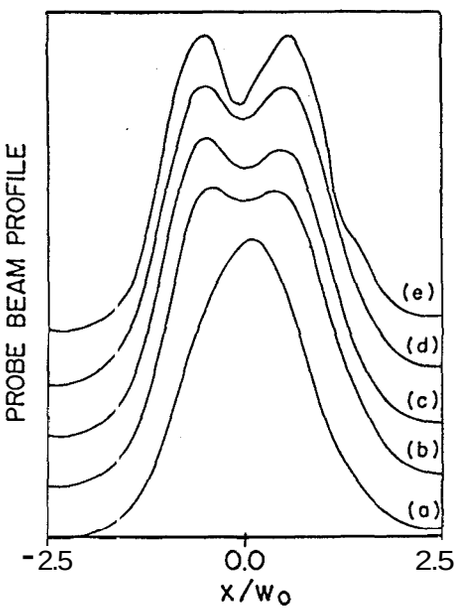

Figure 5.: Transverse probe beam profile after propagation through the sample in the presence of the pump beam. The centers of the two copropagating beams are coincident. Pump intensities: (a) 0; (b) $28kW$; (c) $56kW$; (d) 84kW (e) $112kW$.

Figure 5 shows the weak beam profile when it is exactly overlapped with the strong beam as a function of pump beam power. As predicted in ref.[21], when the pump beam is present the probe spreads but unlike in Figure 4, simmetrically displaced lateral spatial lobes at $\pm 0.5W_0$ are observed when the pump beam power is $112kWatts$. This is, to our knowledge, the first observation of such an effect which is the spatial equivalent of ref.[15] for the time domain. Detection of larger peak separation was linuted by the available power. In this situation the probe is too weak and does not influence the pump beam in a significative way. Figure 6 shows the probe beam profile when the beams are overlapping partially. As can be observed, a profile "compression" (focusing) of the probe beam by a factor of 2 occurs and a shift of $0.5W_0$ was measured. The focusing of the

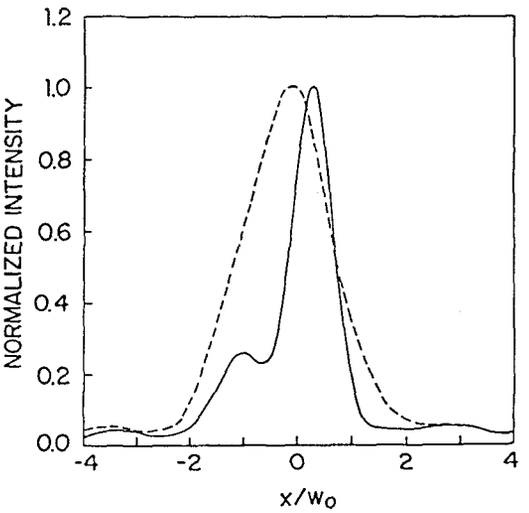

Figure 6.: Transverse probe profile after propagation through the nonlinear medium without the pump beam (dashed line) and with the pump beam (solid line). The beams copropagate along the sample and the overlap occurs only in the wings of the beams profile.

probe beam occurs, as mentioned before, as a result of the XPM induced phase-shift imposed on the probe by the pump. It is important to notice that, for the same conditions, the pump beam exhbits self-defocusing as illustrated in Figure 4. This effect is related in nature to the self-bending effect [11,12] since both arise from the Kerr nonlinearity. Notice however that in our case the underlying physical mechanism exploits the XPM between two beams rather than a self-action process. The oscillatory wing in Figure 6 is the spatial analog of optical-wave-breaking [17].

Figure 7 shows the results of a further experiment performed to demonstrate the potential of the herein reported effects to applications of spatial beam deflection modulation. The results presented show the occurrence of spatial deviation of the probe beam due to the presente of two strong beams overlapping with the probe in its right and left wings respectively. In this experiment the two strong beams at $532nm$ were obtained splitting the original pump in two bemas having equal intensities. Figure 7(a) shows the transmitted probe profile in the absence of the pump beams. Again, no self-action occurs because the probe beam intensity is kept as small as in the other experiments. Figures 7(b) and 7(c) illustrate the probe spatial shift induced by each pump beam when the other is blocked. Notice the spatial shift of $\sim \pm 0.25W_0$ for the right and left of the original probe direction obtained with a peak power of 30kW in each pump beam. In Figure 7(d) we show that it is possible to compensate for either deviation when the two pump beams are simultaneously present. Since the pump beams have equal intensities the probe is no more shifted from its original direction exhbit-

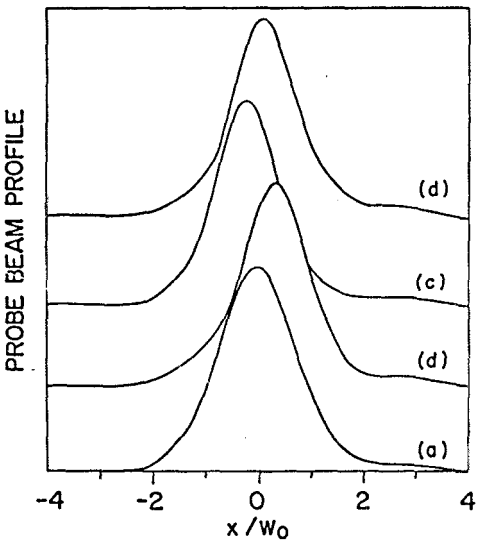

Figure 7.: Probe beam deflection modulation. In (a) only the probe beam is present. For (b) and (c) the overlap between the probe and pump bearns is occuring either in the right or the left wings of the probe. In fig. (d) it is shown that the probe beam returns to its original direction when the right and left pump beams are simultaneously present.

ing a small "compression". This effect can be seen as the formation of an all-optical channel waveguide induced by XPM from two pump beams on a probe beam, and proper control of the pump power should allow the propagation of self-trapped beams.

In conclusion, we have demonstrated the novel phenomena of induced focusing and spatial modulation instability occurring in a self-defocusing medium due to the XPM effect. The phenomena are quite general and can be observed in any material media exhbiting a large Kerr nonlinearity. The possibility of spatial light modulation in the picosecond regime was also demonstrated. The reported effects can be further exploited for studies of logic operations for optical computing.

An extended version of the present work including numerical simulations corresponding to the actual parameters of $Cd(S,Se)$ doped glasses, will be submitted for publication elsewhere.

Acknowledgments

This work was partially supported by the Brazilian agencies: Financiadora Nacional de Estudos e Projetos (FINEP), Conselho Nacional de Desenvolvimento Científico e Tecnológico (CNPq) e Fundação de Amparo à Pesquisa de Pernambuco (FACEPE). We also thank G.P. Agrawal for clarifying discussions.

References

1. A. E. Siegrnan, *Lasers* (University Science Books, Mill Valley, 1986).
2. S. A. Akhmanov, A. P. Sukhorukov and A. S. Chirkin, Sov. Phys. Lett. 28, 748 (1969).
3. E. B. Treacy, IEEE J. Quantum. Electron &E-5, 454 (1969).
4. See, for instance, special issue of J. Opt. Soc. Am. B on transverse instabilities, Vol. B7, 1990.
5. A. Hasegawa and F. Tappert, Appl. Phys. Lett. 23, 142 (1973).
6. L. F. Mollenauer, R. H. Stolen and J. P. Gordon, Phys. Rev. Lett. 45, 1095 (1980).
7. R. Y. Chiao, E. Garmire and C. H. Townes, Phys. Rev. Lett. 13, 479 (1964).
8. A. Barthelemy, S. Maneuf and C. Froehly, Opt. Commun. 55, 201 (1985).
9. For an excellent text in nonlinear pulse propagation in fibers, see G. P. Agrawal, Nonlinear *Fiber Optics*, (Academic Press, Boston, 1989).
10. J. S. Aitchison, A. M. Weiner, Y. Silberberg, M. K. Oliver, J. L. Jackel, D. E. Leaird, E. M. Vogel and P. W. E. Smith, Opts. Lett. 15, 471 (1990).
11. A. E. Kaplan, JETP Lett. **9,** 33 (1969).
12. G. A. Swartzlander, Jr., H. Yin and A. E. Kaplan, Opt. Lett. 13, 1011 (1988).
13. R. R. Alfano, P. L. Baldeck, P. P. Ho and G. P. Agrawal, J. Opt. Soc. Am. B6, 824 (1989).
14. G. P. Agrawal, P. L. Baldeck and R. R. Alfano, Phys. Rev. A, 40, 5063 (1989).
15. G. P. Agrawal, Phys. Rev. Lett. 59, 880 (1987).
16. E. J. Greer, D. M. Patrick, P. G. J. Wigley and J. R. Taylor, Opt. Lett. 15, 851 (1990).
17. G. P. Agrawal, P. L. Baldeck and R. R. Alfano, Opt. Lett. 14, 137 (1989).
18. A. J. Stentz, M. Kauranean, J. J. Maki, G. P. Agrawal and R. W. Boyd, Opt. Lett. 17, 19 (1992).
19. R. de La Fuente, A. Barthelemy and C. Froehly, Opt. Lett. 16, 793 (1991).
20. G. P. Agrawal, Phys. Rev. Lett. 64, 2487 (1990).
21. G. P. Agrawal, J. Opt. Soc. Am. B 7, 1072 (1990).
22. L. H. Acioli, J. Miguel Hickmann, A. S. L. Gomes and Cid B. de Araújo, Appl. Phys. Lett. 56, 2279 (1990).
23. G. R. Olbright and N. Peyghambarian, Appl. Phys. Lett. 48, 1184 (1986).
24. P. Roussignol, D. Ricard and C. Flytzanis, Appl. Phys. A44, 285 (1987).
25. H. Ma, L. H. Acioli, A. S. L. Gomes and Cid B. Araújo, Opt. Lett. 16, 630 (1991).